Comparative studies on control systems for a two-blade variable-speed wind turbine with a speed exclusion zone

Yang, Jian; Song, Dongran; Dong, Mi; Chen, Sifan; Zou, Libing; Guerrero, Josep M.

Published in:
Energy

DOI (link to publication from Publisher):
10.1016/j.energy.2016.04.106

Publication date:
2016

Document Version
Early version, also known as pre-print

Comparative study on the control systems for a two-blade variable-speed wind turbine with a speed exclusion zone

Jian Yang[1], Dongran Song[1,2], Mi Dong[1,*], Sifan Chen[2], Libing Zou[2], Josep M. Guerrero[3]
[1]School of Information Science and Engineering, Central South University, Changsha, P.R. China
[2]Chinese Ming Yang Wind Power Group Co., Ltd., Zhongshan, P.R. China
[3]Microgrid Research Programme, Dept Energy Technology, Aalborg University, Denmark

ABSTRACT
For a two-blade wind turbine with a full rated converter, a speed exclusion zone (SEZ) has to be built up to avoid the coincidence between tower nature frequency and rotational frequency. In this paper, two control systems are developed to perform power generation tasks at the same time bypassing SEZ. The paper focuses on comparative study on their operation strategies and performance of the developed control systems. Three operation strategies including power optimization, power limitation and power regulation, are presented, whereas optimal designs are introduced to improve existing SEZ algorithms as well as solving their problem. Besides, two separated operation modes are divided in the proposed down power regulation solutions to perform power regulation outside the SEZ. The performance of the control strategies are evaluated through simulations and field testing. The two control systems present similar capabilities of power production and SEZ-bridging. However, when compared with the control system 1, the control system 2 is capturing 1% more energy under normal grid regulation and even more energy under down power regulation, but at the cost of significantly increased tower loads.

KEYWORDS
Two-blade variable speed wind turbine, control system, speed exclusion zone, tower resonance, power capture, tower loads.

Correspondence
Mi Dong, School of Information Science and Engineering, Central South University, Changsha, P.R. China.
Email: mi.dong@csu.edu.cn

NOMENCLATURE

θ_{set} , θ_m	the pitch angle set-point of the pitch controller and measured pitch angle.
w_A , w_B , w_C , w_D	four speed points at optimum tip speed section.
w_b , w_c	the lower and higher speed boundary of the speed exclusion zone.
w_o	the critical speed corresponding to the resonance frequency.
w_{r_pl} , w_{r_ph}	the speed reference of the pitch controller on low power mode and high power mode
w_{r_p}	the speed reference of the pitch controller
w_{r_tl} , w_{r_th}	the speed reference of the PI torque controller on low power mode and high power mode
w_{r_t}	the speed reference of the PI torque controller
w_{r_m}	the measured rotor speed
T_{opt}	the optimal torque
P_{set}	the power command ordered from wind farm controller
P_{rated}	the rated power
P_{set_b}	the set-point power to the boost converter controller
P_{l_l} , P_{l_h}	the set-point power from the look-up torque controller on low and high power mode
P_l	the set-point power from the look-up torque controller
P_B , P_C	the power set-points at rotor speed w_B and w_C
P_E , P_F	the upper and lower power limits at the speed boundary w_b and w_c
P_{l1} , P_{l2} , P_{l3}	three power limits at the speed boundary w_c
P_{h1} , P_{h2} , P_{h3}	three power limits at the speed boundary w_b
Mx, My, Mz	the roll moment, nodding moment, and yawing moment

1. INTRODUCTION

Modern wind turbine (WT) is variable-speed and with flexible structure. In order to capture wind energy and decrease the mechanic loads to the greatest degree, it is required that WTs have a wide variable-speed operation region. However, a wide operation region makes it possible that the rotor rotary frequency and the natural frequencies of other structural components are coincident at some certain rotor-speed. In order to eliminate the underlying resonance, some preventive measures are normally performed during the design phase, including natural characteristics calculations and potential resonance problem analyses [1]. During the concept design phase, it is taken into consideration that not only is certain gap reserved among natural frequencies of blades, tower, and driver train, but also the coincidences among natural frequencies and external resonance force are mostly avoided [2]. It is recommended that the eigenfrequency of rotor blade is outside a 12% range of the rotational frequency of the WT, and the tower lowest mode frequency is kept outside ranges defined as $\pm 10\%$ the rotor frequency and $\pm 10\%$ the blade passing frequency, respectively [3]. In practical application, the problem caused by tower resonance is especially significant, since tower resonance results in vibrations of the whole WT set and directly affects the WT's safety. For a three-blade WT, it is possible to change the natural frequency and place it in the region between 1P and 3P through redesigning tower's thickness and radius. But for a two-blade WT, it will bring about greatly increased cost to change tower's natural frequency lower than 1P or higher than 2P. Therefore, the only feasible way to prevent the WT operating in the speed exclusion zone (SEZ) is to redesign the control system.

The control algorithms for the WT with a SEZ have been described in previous works [4]-[9]. Among these works, two control approaches can be distinguished. The approach one, first recorded in [4], is based on a conventional look-up table torque control method. The approach two, proposed in [5]-[7], is developed on the basis of a PI torque control method. In both approaches, one certain speed region, including the critical speed and its neighbor speed points, is built up to form a SEZ. These two approaches differ in the establishing and bridging-over way of the SEZ. The principle in the first approach is to create an ambiguous function between rotor speed and generator torque, so that the generator can accelerate to cross the SEZ through an unbalance relation between aerodynamic torque and demanding generator torque. The second approach is to gradually ramp the speed reference of the PI speed controller from one fixed speed boundary to the other. Despite the two approaches available, studies about their applications in real wind turbine are few. As far as we know, only in [8], different widths of SEZ based on the second approach were investigated and validated on a 1.3kW test rig. Besides, in [9], we employed the first approach into the control system design of a two-bladed WT. In wind energy industry, the control strategy validation through field trials is vital and not substituted. After field trials, the underlying problem can be revealed. Based on data analysis to the field testing results, two drawbacks are found for the control approach applied in [9]: one hand, the experimental turbine fails to cross over the SEZ under certain wind conditions; on the other hand, the power capture performance is not satisfactory. Therefore, optimization technique needs to be further investigated. Besides, the performances of the available control approaches are not studied in references, which is vital for the WT designers and owners to make decision on the control system selection for the WT with the SEZ.

The above-discussed control strategies only refer to control subject of conventional control system, which is to maximize power production while maintaining the desired rotor speed and avoiding equipment overloads [10]. Nowadays, the wind farms are required to participate actively in the power system operation as conventional power plants [11]. As a result, WTs are required to regulate power according to the power set-points ordered by the central control systems of wind farm. Thus, recent WTs' control systems have to perform three operating strategies: power optimization strategy, power limitation strategy, and power regulation strategy. These three power generation tasks are fulfilled in a certain operation region constrained by the rotor speed. In the case of a WT with no SEZ, it is only necessary to limit the rotor speed to the speed reference by the pitch controller under power limitations. Up to now, many works have contributed to the control system study of generic WTs, especially to the doubly fed induction generator WTs [12]-[16]. When considering the WT with a SEZ, unique control strategy has to be concerned with performing power

generation while maintaining the rotor speed outside the SEZ. However, it is lacking of references on such kind of WTs.

The main purpose of this work is to perform a comparative study of two control systems for a two-bladed WT with a SEZ. Firstly, two control systems capable of fulfilling three operation tasks, including power optimization, power limitation and power regulation, are developed. The control system 1 is based on a look-up table, whereas the control system 2 is based on a PI torque control method. In order to improve conventional methods and solve their uncertainties of SEZ-crossing under different wind conditions, optimization techniques are presented. Meanwhile, considering power regulation requirements from grid operators, simple but practical power regulation strategies are proposed to fulfill power regulation task at the same time bypassing the SEZ. Afterwards, a comparative study of the control strategies on both performances of power capture and fatigue loads, is performed by means of detailed non-linear simulations and field tests.

2. THE STUDIED TWO-BLADE WT

2.1. Basic information

The target WT is a two-blade 3.0 MW super compact drive machine. It is manufactured by Chinese Mingyang Wind Power Company and its specification is shown in Table. 1.

Table. 1. Specification of the studied WT

Parameters	Value
Rotor diameter	110m
Number of rotor blades	2
Rated electrical power	3000kW
Rotor speed range	6.0-21.0rpm
Nominal rotor speed	16.2rpm
Rated wind speed	12.2m/s
Rotor moment of inertia	$1.5\times10^{7} kg\cdot m^{2}$
Generator moment of inertia	$2.1\times10^{3} kg\cdot m^{2}$
Gearbox ratio	23.94
Cut-in wind speed	3m/s
Cut-out wind speed	20m/s

The WT is with a super compact structure, and its main body can be regarded as two parts: energy conversion part and its supporting structure-a tubular steel tower. The simplified topological structure of the energy conversion part is shown in Fig. 1, including a blade rotor, a low ratio gearbox, a permanent magnet synchronous generator (PMSG) and a full-scale power converter.

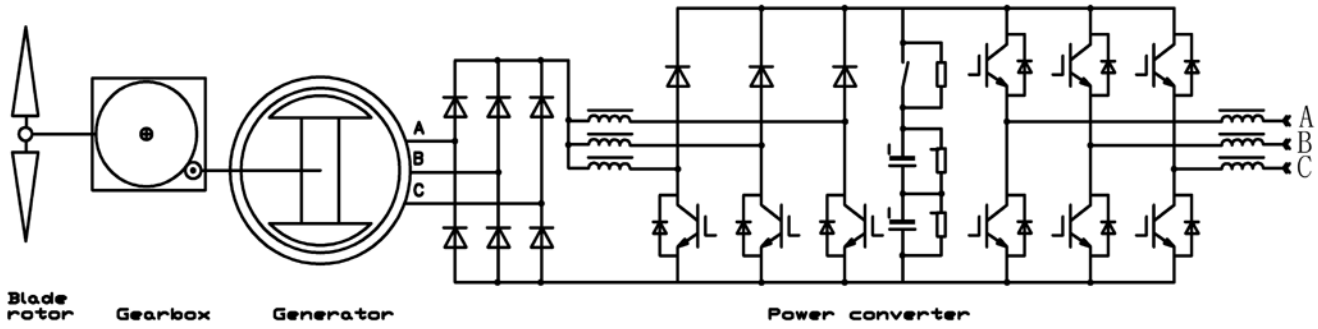

Fig. 1. The topological structure of energy conversion part of the studied WT.

2.2. Characteristic curves of the target WT

By using the Bladed software [17], the characteristic curves of the target machine are obtained.

Both of aerodynamic power coefficients (Cp) and thrust coefficient (Ct) curves of the target WT are shown in Fig. 2. Generally, the pitch angle and tip speed ratio (TSR) for maximum Cp acquisition are called as optimal pitch angle and optimal TSR, respectively. In Fig. 2, the maximum Cp is 0.454486, and the corresponding optimal pitch angle and the optimal TSR are 0 degree and 10.5, respectively. Meanwhile, it can be seen that the optimum pitch angle is changing in the range of -1deg-1deg along with the variation of TSR in the range of 8-12. Besides, we get to know that Ct increases along with the decreasing pitch angle when TSR is constant. According to [18], the tower loads is proportional to the thrust coefficient. Therefore, regarding tower loads, it is beneficial to keep a large pitch angle and a lower TSR.

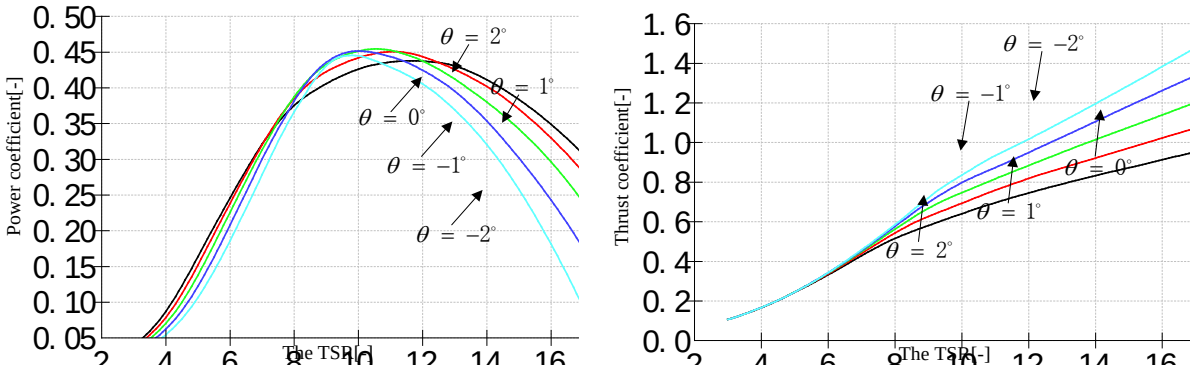

Fig. 2. The studied WT's aerodynamic power coefficient and thrust coefficient curves.

Finally, Fig. 3 shows the natural frequencies of the low frequency structural mode shapes of the studied turbine as a function of rotor speed. It is obvious that the blade passing frequency 2P and the lowest two tower mode frequencies are consistent at the rotor speed of 10rpm. Therefore, there is a SEZ for the studied WT, which is built up by the control systems studied in this work.

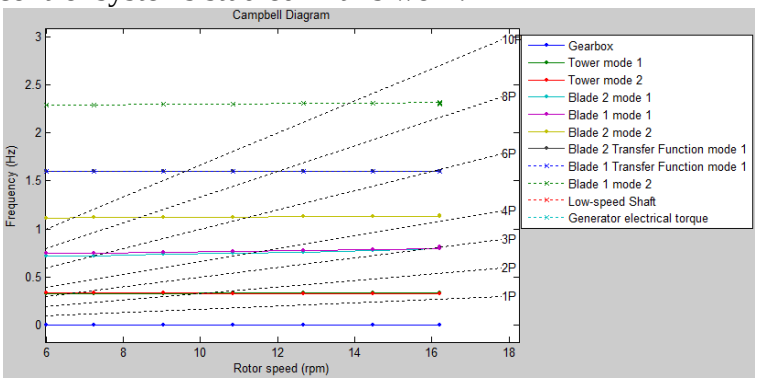

Fig. 3. The Campbell diagram of the studied WT.

2.3. Control system architecture of the studied WT

The control system of a modern WT is usually divided into two control levels, the generator control level and the WT control level. These two control levels are distinguished with different bandwidths [14]. For the studied turbine, a consolidation control architecture is adopted, which incorporates the major control elements for running a WT as well as ensuring that energy from power converters has been injected into electricity network at maximum efficiency [19]. Fig. 4 illustrates the control system architecture. The Siemens IPC P320 is used as the control unit. Based on the Profinet protocol, the power converter and major control components are controlled by the same controller within two task periods of 250us and 10ms, respectively. With this consolidated architecture, the relation and constraint between different control levels become quite clear. Therefore, it turns out to be quite convenient to implement control algorithms for the WT.

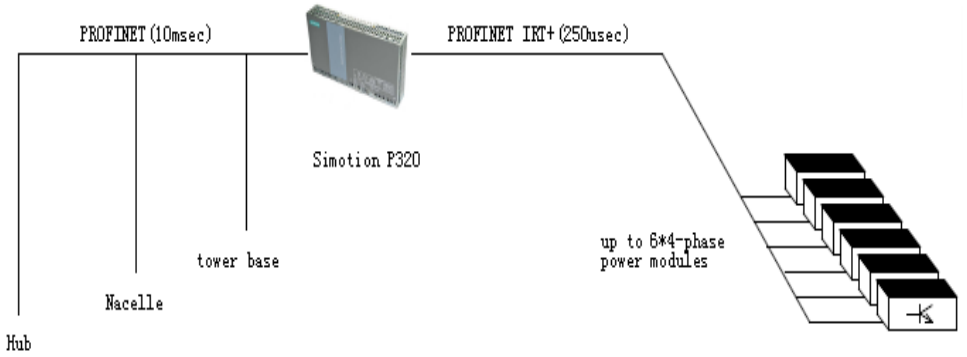

Fig. 4. The control system architecture of the studied WT.

3. THE OPERATION STRATEGIES OF THE STUDIED WT

From the power generation system point of view, there are three operation tasks for modern WTs [16]:

- limit the output power to the rated power for high wind speeds (power limitation condition);
- maximize the power extracted from the wind for a wide range of wind speeds (known as power optimization condition);
- adjust both active and reactive powers to a set-point ordered by the wind farm control system (power regulation).

When completing these three tasks, it is a prerequisite to maintain the rotor speed in the predefined range. Otherwise, the machine would suffer from overload. For a generic WT with no SEZ, its rotor speed is controlled within a continuous operation zone limited by the cut-in speed and the rated speed. But for the WT with a SEZ, besides constrained by the cut-in and rated one, its rotor speed has to be held away from the critical speed. Separated by the SEZ, there are two operation zones: the low speed zone and the high speed zone. For this kind of WTs, the existence of the SEZ affects their power optimization and power regulation operation. As the purpose of this work is to study the control systems of the WT with SEZ, controls unaffected by SEZ will be shortly described or left out for the sake of simplicity. The common operation strategies employed by the control systems are summarized as follows:

- in power limitation condition, the operation strategy for the studied WT is mainly in the charge of the pitch controller. The rotor speed is controlled to the rated value by the pitch controller and the generator torque is limited close to the rated torque by the boost converter. As illustrated in Fig. 5, the pitch controller includes three main parts: a PD controller and two fuzzy logic units. For the PD controller, its input is the error between the reference rotor speed w_{r_p} and the measured rotor speed w_{r_m}, and its output is the pitch speed set-value to the hydraulic proportional valves. Two fuzzy logic units, FC1 and FC2, are designed for the pitch bias determination and over-speed problem prevention [20], respectively.

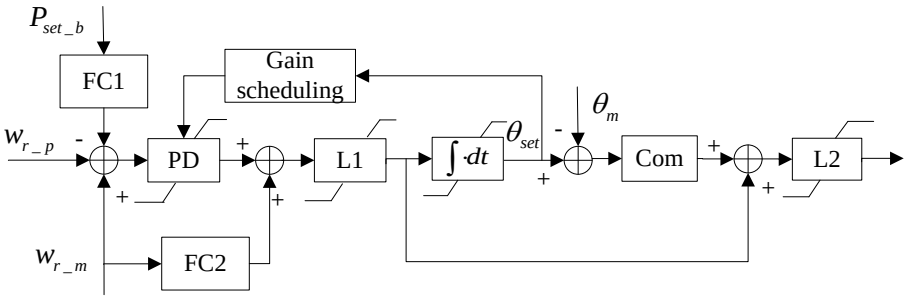

Fig. 5. The structure diagram of the pitch controller.

- in power optimization condition, the torque controller is responsible for the optimized operation and the pitch angle is kept at its optimal value by the pitch controller. Under this case, the rotor speed is controlled by the torque controller not only to track the optimum TSR outside the SEZ, but also to cross over the SEZ.

- in power regulation condition, the operating strategy requires the cooperation between the pitch controller and the torque controller. According to [16], three control strategies are available for DFIG WTs with no SEZ. Recalling that down power regulation mainly involves in the calculations for the power and rotor speed set-points, these control strategies can be also employed by the control system of PMSG WTs. However, spe**c**ial down power strategy has to be concerned.

4. THE CONTROL SYSTEMS OF THE STUDIED WT

As aforementioned, two control approaches are distinguished for the WT with a SEZ under power optimization operation in previous works. Based on these two control approaches, two control systems (denoted as control system 1 and 2) are developed for the studied WT. The control system 1 is based specifically on [9], whereas the control system 2 is based on [8]. Meanwhile, optimal techniques are presented to improve the conventional SEZ-crossing methods. Furthermore, power regulation strategies are proposed to complete the two control systems under down power regulation operation.

4.1. Control system 1

4.1.1. Control system 1 structure

The structure of control system 1 is illustrated in Fig. 6, including four main parts: the pitch controller and its speed reference calculation, the boost converter controller and its power set-point calculation.

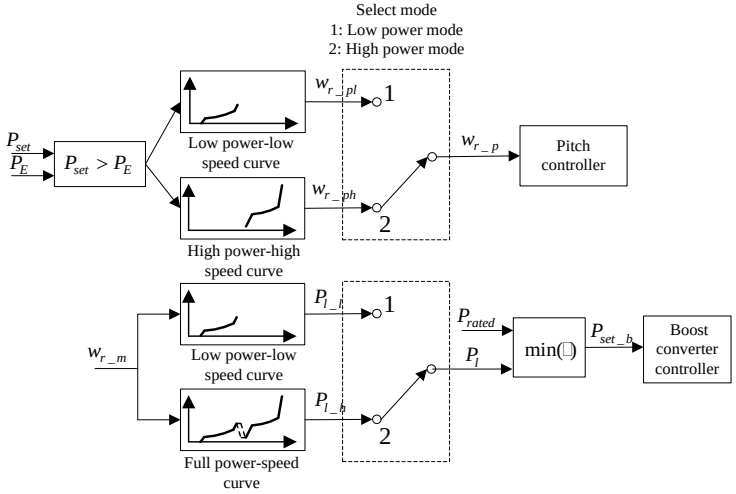

Fig. 6. The control system 1 structure.

Based on Fig. 6, the operation strategies are summarized as follows:

- power limitation strategy: the speed reference w_{r_p} for the pitch controller is the rated value, and the power set-point P_{set_b} for the boost converter controller is calculated based on the full power-rotor speed curve and the measured rotor speed w_{r_m}.
- power optimization strategy: the pitch angle is kept at its optimal value by the pitch controller, and the rotor speed is controlled by the torque control strategy explained as follow.
- power regulation strategy: the down power regulation strategy is divided into two power operation modes: low power operation mode and high power operation mode. These two modes are determined by the power command P_{set} from wind farm controller, and the power division point P_E, which corresponds to the upper power limit at the lower speed boundary of the SEZ. When P_{set} is not larger than P_E, the WT operates on low power operation mode: w_{r_p} takes w_{r_pl} calculated from the low power-low speed curve and P_{set}, while P_{set_b} is calculated from the low power-low speed curve and w_{r_m}. Otherwise, the WT operates on high power operation mode: w_{r_p} takes w_{r_ph} calculated from the high power-high speed curve and P_{set}, while P_{set_b} is calculated from the full power-speed curve and w_{r_m}.

4.1.2. The optimized torque control scheme in control system 1

The torque control scheme is illustrated in Fig. 7, including three parts: the power set-point calculation, the bias unit, and the boost converter controller.

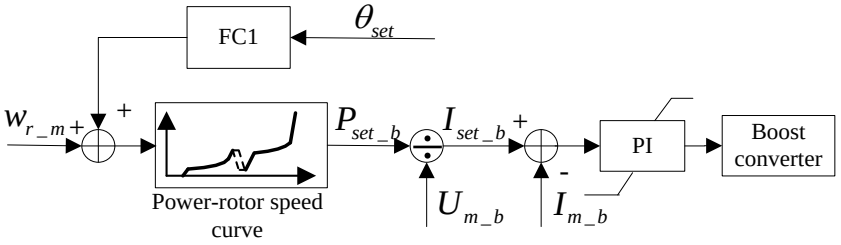

Fig. 7. The torque control scheme in the control system 1.

The boost converter controller employs a PI controller to control the boost current to the set-point I_{set_b}, which is calculated by dividing the power set-point P_{set_b} with the rectifier DC-voltage U_{m_b}. The bias unit FC1 is to decouple the pitch controller and the torque controller. The power set-point calculation determines the parameters of the power-rotor speed look-up table, which includes normal points predefined according to the aerodynamic data of the WTs' rotor, and the special points related to the SEZ. In this work, eight pairs of power-rotor speed points are used in the look-up table and their parameters are shown in Table. 2. In [9], we proved that for a two-blade WT, proper widths of the SEZ and its neighbor zones can be $\pm 10\%$ .Here, the SEZ is preset in 9rpm-11rpm, its two neighbor zones are defined in 8.2rpm-9 rpm and 11rpm-11.9rpm, and the upper and lower power limits at two speed boundaries of the SEZ are 18% and 2%, respectively.

Table. 2. The power-rotor speed lookup table

Measured value of rotor speed (rpm)	Power set-point (100%)
6.0	0.0
8.2	8.0
9.0	18.0
11.0	2.0
11.9	17.0
13.7	35.0
15.0	48.0
16.2	100.0

In order to enhance the SEZ-bridging capability under different wind conditions, we present a hysteresis technique to replace the predefined power-rotor speed points within the SEZ. As illustrated in Fig. 8, the technique is described as: when the rotor-speed is increased above the lower speed boundary $w_b(9.0rpm)$, the power set-point P_{set_b} is decreased with certain rate to the end point of $P_F(2.0\%)$; when the rotor-speed is decreased bellow the higher speed boundary $w_c(11.0rpm)$, the power set-point is increased with certain rate to the end point of $P_E(18.0\%)$.

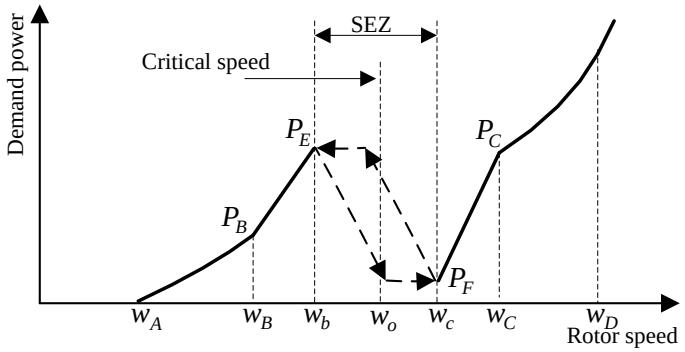

Fig. 8. The optimized SEZ-crossing technique in control system 1.

4.2. Control system 2

4.2.1. Control system 2 structure

Similar to control system 1, control system 2 also includes four main parts: the pitch controller and its speed reference calculation, the boost converter controller and its power set-point calculation. Its structure is illustrated in Fig. 9.

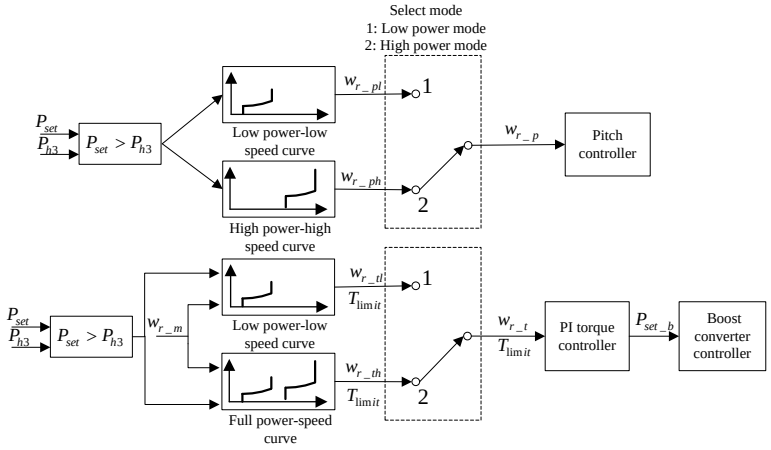

Fig. 9. The control system 2 structure.

Based on Fig. 9, the operating strategies for the control system are the followings:

- power limitation strategy: both speed references of the pitch controller and the PI torque controller are the rated value. As a result, the rotor speed is maintained at the rated speed by the pitch controller and the torque demand is limited to the rated value by the torque controller.
- power optimization strategy: the pitch angle is kept at its optimal value by the pitch controller, and the rotor speed is controlled by the PI torque control strategy.
- power regulation strategy: the speed reference w_{r_p} of the pitch controller and the power set-point P_{set} of the boost converter controller are derived based on the two power operation modes as mentioned earlier. On low power mode, w_{r_p} takes w_{r_pl}, which is derived from the low power-low speed curve and P_{set}. On high power mode, w_{r_p} takes w_{r_ph}, which is calculated from the high power-high speed curve and P_{set}. Meanwhile, P_{set_b} is calculated from the output of the PI torque controller and w_{r_m}.

4.2.2. The optimized torque control strategy in control system 2

The torque control strategy is illustrated in Fig. 10 and also includes three parts: the power set-point calculation, the bias unit, and the boost converter controller. The boost converter controller and the bias unit are same as those in the control system 1. The power set-point calculation refers to a PI torque controller and a mode selection unit.

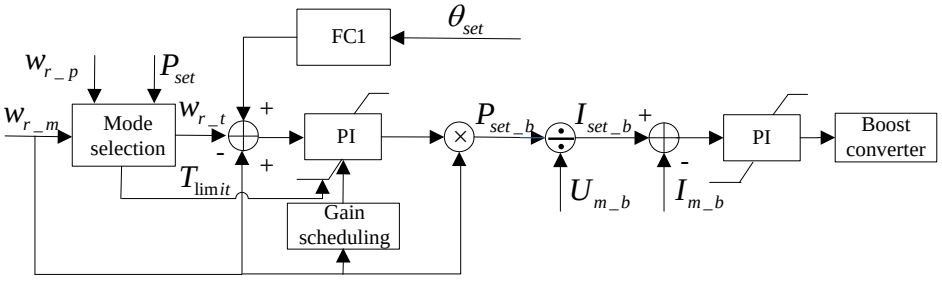

Fig. 10. The torque control scheme in control system 2.

The design of PI controller is a routine with the assistance of Bladed software, and its parameters are given as: $k_p = 8300.0$, $k_i = 1300.0$, and the gain scheduling factor is 1.5. Besides, the optimal torque T_{opt} is calculated by $T_{opt} = kw_{r\_m}^2$ [21]. For the target turbine, $k = 14322$.

The mode selection unit in charge of the SEZ algorithm is to calculate the speed reference and torque limits for the PI torque controller. In order to carry out comparison to the control system 1, the SEZ with same range of 9rpm-11rpm is preset. Based on the PI torque controller, the power-rotor speed characteristic curve of the WT is shown in Fig. 11.

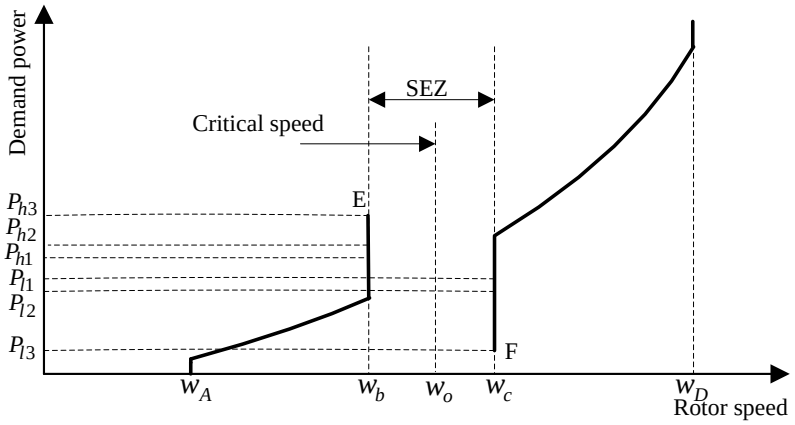

Fig. 11. Power–rotor speed curve in control system 2.

In the mode selection unit, the speed reference and the torque limits are calculated based on three operating modes: low speed mode, the SEZ mode, and high speed mode. The rotor speeds at the low speed mode, the high speed mode, and the SEZ mode are in the range of $w_A - w_b$, $w_c - w_D$, and $w_b - w_c$, respectively. The basic strategy is summarized as: at the low speed mode, when the rotor speed is smaller than $(w_A + w_b)/2$, the speed reference is set to w_A, then generator torque adjusts the rotor speed to achieve the optimal TSR; whereas if the rotor speed increases and becomes larger than $(w_A + w_b)/2$, the speed reference changes to w_b, then generator torque controls the rotor speed to vary up to w_b. When the wind speed increases, the rotor speed is held close to w_b by the increasing generator torque. Once the transition condition is satisfied, the WT starts transiting to the SEZ mode. And at the SEZ mode, a ramping speed reference is performed by the controller until it passes the SEZ. The transition from high speed mode to low speed mode operates in a similar way.

In order to successfully cross the SEZ under various winds, a variable transition technique is employed. This technique ensures three types of transition: long time transition, medium time transition, and short time transition. As illustrated in Fig. 11, at low speed mode and high speed mode, long time transitional conditions are averaged output power of long time, medium time, and short time more than P_{h1} and less than the P_{l1}, respectively; medium time transitional conditions are averaged output power of medium time and short time more than P_{h2} and less than the P_{l2}, respectively; and short time transitional conditions are averaged output power of short time more than P_{h3} and less than the P_{l3}, respectively. For the studied WT, the three hysteresis time: long time, medium time, and short time, are 5m, 30s, and 3s, respectively; the upper power limits P_{h3}, P_{h2}, and P_{h1} are 540kW, 440kW, and 410kW, respectively; and lower power limits P_{l3}, P_{l2}, and P_{l1} are 200kW, 325kW, and 350kW, respectively. Besides, the crossing time is 15s for long and medium time transition, and 10s for short time transition.

5. PERFORMANCE COMPARISONS OF TWO CONTROL SYSTEMS

5.1. Comparative study based on simulation results

In this work, two purposes are fulfilled through detailed simulations with Bladed: the control algorithms validation and the performance comparisons in the aspects of structure loads and power production. In order to enhance the power capture performance, the control algorithm in control system 2 is further improved by limiting the pitch controller's output at the optimum pitch angle based on the Cp curves shown in Fig. 2. Therefore, three controllers are developed as external dynamic library. Controller 1, controller 2 and

controller 3 refer to control algorithm 1 (in control system 1), control algorithm 2 and the updated control algorithm 2 (in control system 2), respectively. Regarding the fact that the simulation running time is comparatively shorter than the operation time of the real WT, the hysteresis time employed by controller 2 and controller 3 is shorten to 1m, 10s, and 1s in simulations.

5.1.1. The validation of the proposed control algorithms

Regarding the control algorithms focusing on the controls related to the SEZ, two operation scenarios are assumed: power optimization operation and power regulation operation. In order to validate the effectiveness of the developed controllers, 13 simulation tests are implemented, which are preset by two operation scenarios with single point history and 3D turbulent winds. The single point history winds are set to step winds from 3m/s-12m/s, and 3D turbulent winds are defined with mean wind speed of 6m/s and three typical turbulence intensities of: 14%, 16%, and 18%. In this work, for the sake of simplicity, only two representative simulation results are chosen to show, which are based on one power optimization case and one power regulation case with 16% turbulence intensity winds. Among numerous simulation results obtained from the Data View menu of Bladed, six measurable signals are shown: wind speed, rotor speed, output electrical power, pitch angle, nacelle side-side and fore-aft accelerations. Black curves, red curves, and green curves are drawn for the simulation results from controller 1, controller 2, and controller 3, respectively.

The simulation results from the power optimization case are illustrated in Fig. 12a. It is clear that all three controllers succeed in building and crossing over the SEZ. However, three differences are obvious. Firstly, times of crossing the SEZ are different. Three times of crossing over the SEZ happen for controllers 2 and 3, whereas there is only once for controller 1. Secondly, before and after crossing the SEZ, the rotor speeds of WT with controllers 2 and 3 are maintained closer to the speed boundaries of the SEZ. Thirdly, except several points, the nacelle accelerations of the WT with controller 1 are slightly smaller than the ones from controllers 2 and 3. These differences affect the performances of power capture and tower loads, which will be numerically presented in the next section.

In the down power regulation case, the power regulation demand is set to 450kW before 290s, and increases to 550kW at 290s with a ramping rate of 50kW/s. From simulation results illustrated in Fig. 12b, we see that all three controllers succeed in following the power regulation commands at the same time bypassing the SEZ. Meanwhile, four differences are distinguishable. Firstly, times of crossing the SEZ are different: three times happen for controllers 2 and 3, whereas only once for controller 1. Secondly, before and after crossing the SEZ, the rotor speeds of the WT with controllers 2 and 3 are upheld tightly to the speed boundaries of the SEZ, whereas the rotor speed with controller 1 is located in the neighbor zones of the SEZ. Thirdly, both nacelle fore-after and side-side acceleration amplitudes with controller 1 are obviously smaller than those with controllers 2 and 3. Lastly, the pitch controllers are activated at different time points and with different actions when the output power increases up to the power demand. These differences directly affect the WT's performance, which will be also presented in the next section.

5.1.2. Performance comparisons with the simulation results

The numerical results are obtained based on the post processing functions provided by the Bladed software. Three kinds of simulations results are compared. The first two are from the power optimization and power regulation simulation cases in the last section, and the third is from a complete set of simulations with IEC standard [22].

In order to check the WT performance with different controllers, the averaged power production and the equivalent loads of the tower are calculated. The numerical results from Fig. 12a are summarized in Table. 3. We observe that the averaged power production and tower equivalent loads are closer in the results of controllers 2 and 3, while there is a slight increase for power output by controller 3. This result makes a good agreement to the fact that only the pitch angles differ in these two controllers. When compare the results between controller 1 and controller 2 (or controller 3), obvious discrepancies are found. Controller 2 increases the averaged power by about 1.6%, but almost doubles the tower Mx equivalent load and increases My equivalent load by more than 20%.

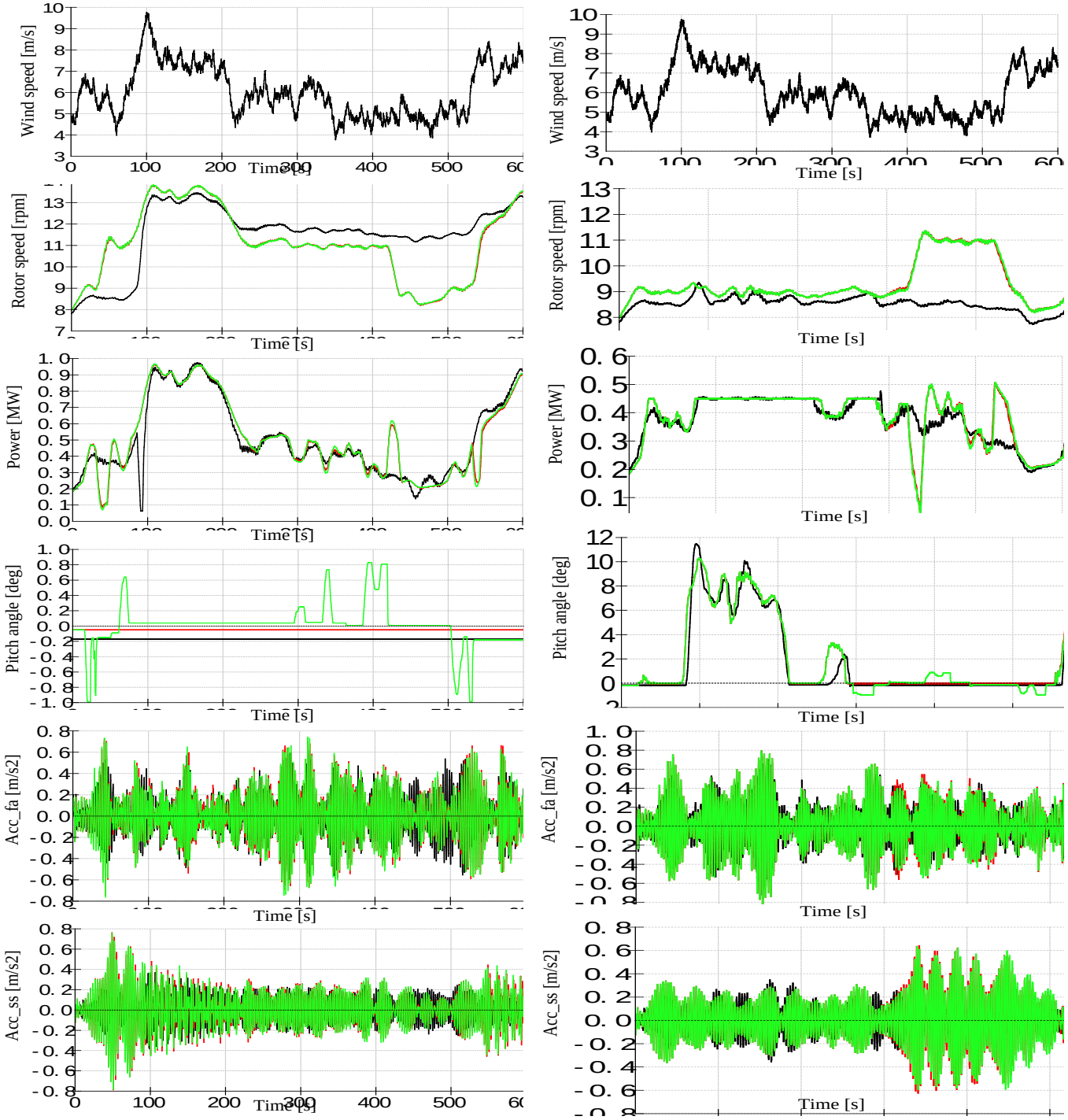

Fig. 12. Simulation results among three controllers: (a) at power optimization case and (b) at deloaded case.

Table. 3. Summarized numerical results from Fig. 12a

Controller	Mx(MNm)	My(MNm)	Mz(MNm)	Averaged power(MW)
1	3.757	7.298	1.103	0.502
2	7.413	8.917	1.066	0.509
3	7.361	8.899	1.066	0.510

For the deloaded case, the numerical results are summarized in Table. 4. In this case, controllers 2 and 3 produce same power and result in similar equivalent tower loads. This fits the fact that the trajectories of the rotor speed and pitch angle in Fig. 12b are almost overlapped in these two controllers. When compared with

controller 1, controller 2 increases the average power by more than 3.1%, yet lifts up the tower Mx and My equivalent loads by more than 85% and 22%, respectively. Since the pitch actions under the power regulation operation directly affect the thrust and therefore the tower loads, these comparative results are different from the ones in Table. 3.

Table. 4. Summarized numerical results from Fig. 12b

Controller	Mx(MNm)	My(MNm)	Mz(MNm)	Averaged power(MW)
1	4.723	9.115	0.805	0.381
2	8.640	10.880	0.973	0.393
3	8.592	10.812	0.972	0.393

In accordance with IEC standard [22], a complete set of simulation series is performed to calculate the design loads, which is essential to evaluate the controller impact on the loads before carrying out the field testing. In the simulation series, different winds are defined based on the analysis of wind resource measurement for the wind farm site where the studied machines are deployed: the annual average wind speed at hub height is 6.42m/s and the characteristic turbulence intensity at 15m/s is 12%. Since the same pitch control algorithm and supervisory control strategy are performed in the three controllers, the fatigue loads rather than extreme loads are mainly affected by the three controllers. Therefore, we focus on the performance comparisons in the aspects of fatigue loads and power production.

The damage equivalent loads (DELs) are calculated based on the assumption that the WT's lifetime is 20 years and the press cycle time is 1.0E+08. Using Wohler exponent 4 (appropriate for steel), the DELs of Four components (blade root, hub, yaw bearing, and tower bottom) with controller 1 are shown in Table. 5. By using the results of controller 1 as the baseline, the comparative results of controllers 2 and 3 are presented in Fig. 13. It is clear that the DELs caused by controllers 2 and 3 are nearly the same, but bigger than those by controller 1. Obvious increases in the tower bottom DELs are caused by controllers 2 and 3: the Mx DEL is increased by nearly 60% and the My DEL by more than 10%. For other components' DELs, less than 5% increases are caused by controllers 2 and 3.

Table. 5. The DELs of four components with SN4

Component	Mx(kNm)	My(kNm)	Mz(kNm)
Blade root	5640.79	2281.65	57.40
Stationary hub	393.36	2491.80	2491.84
Yaw bearing	452.34	2472.33	2482.58
Tower bottom	5003.96	9983.03	2482.45

In order to observe the contributions of different wind speeds to the DELs of the tower bottom, the tower bottom Mx and My DELs of the design load case (DLC) 1.2 are shown in Fig. 14. The tower bottom Mx and My DELs with controllers 2 and 3 almost double the ones with controller 1 at the wind speeds of 4m/s and 6m/s. This is because the rotor speeds with controllers 2 and 3 at the low winds are controlled to the speed boundaries of the SEZ. At wind speeds of 8m/s and 10m/s, the tower bottom Mx DELs are almost equal for the three controllers, while the tower bottom My DELs are increased for controller 2 and controller 3. The reason for this increase is that My is mainly affected by the thrust. The rotor speeds with controllers 2 and 3 are higher than the one with controller 1, and correspondingly the TSRs are lifted up to produce a larger thrust.

Based on the simulation results at DLC 1.2, the averaged power at different wind speeds is calculated. As shown in Fig. 15, the results with controller 1 are taken as the baseline result to compare with the results from controllers 2 and 3. It is very clear that different averaged power is produced by three controllers. By comparison to controller 1, controllers 2 and 3 increase the power production at wind speeds of 8m/s, 10m/s and 12m/s, while decrease the power production at other wind speed. The increased power production at medium wind speed is caused by an optimal TSR tracked by controllers 2 and 3. The less than 0.3% decreased power productions above the rated winds can be explained by the power loss model which is determined by the rotor speed and generated power. But less power production at 4m/s and 6m/s seems

contradicted to the results shown in Table. 3. However, it is understandable to take the influence of different turbulence intensity into consideration.

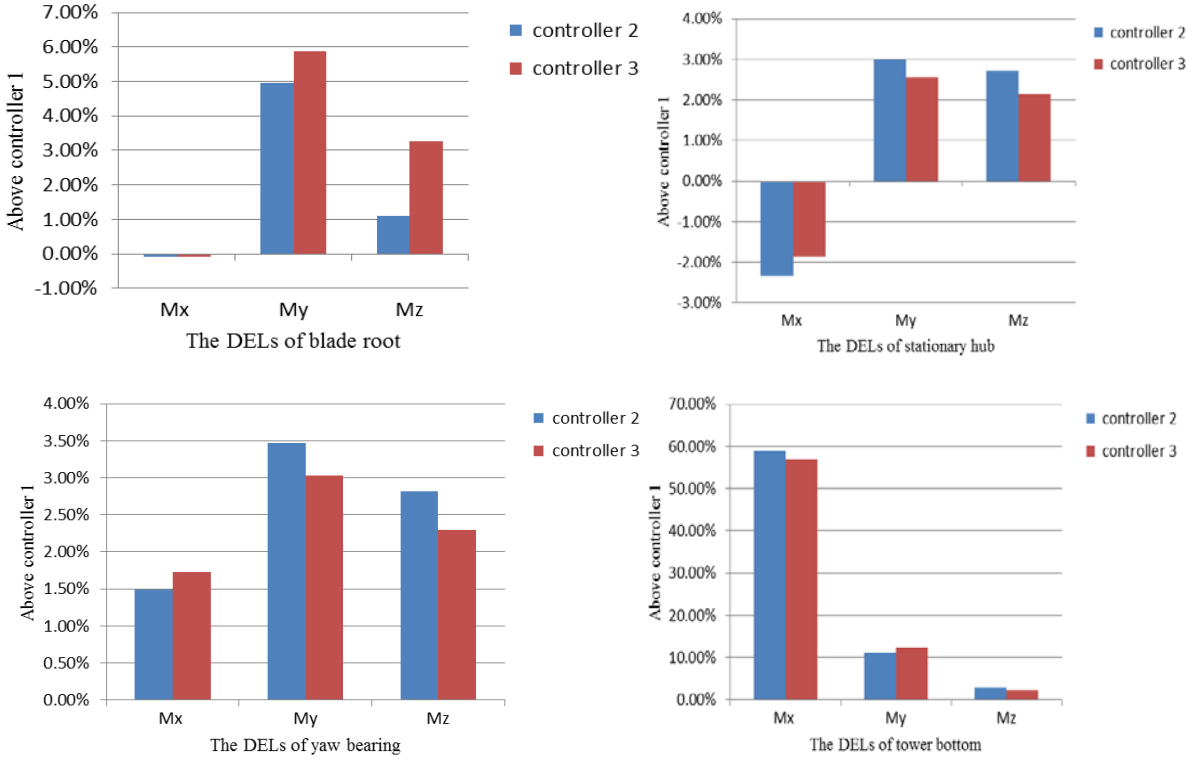

Fig. 13. Four components DELs comparisons among three controllers.

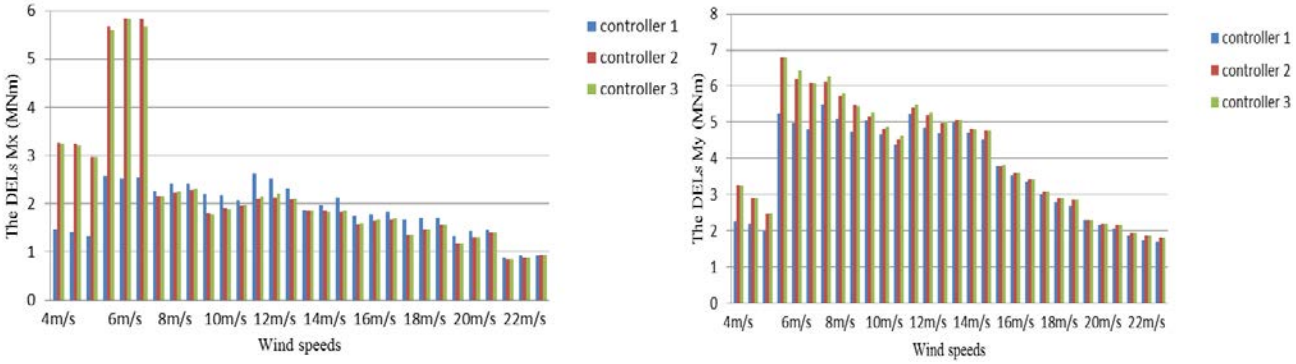

Fig. 14. Comparisons for tower bottom Mx and My DELs at DLC 1.2 among three controllers.

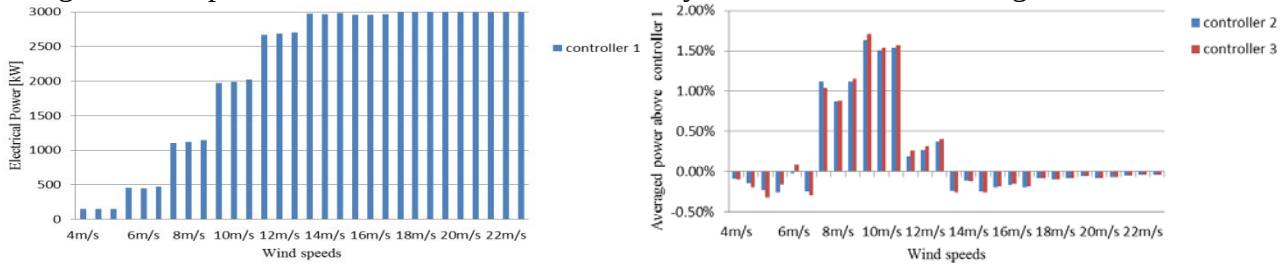

Fig. 15. Averaged electrical power comparison at DLC 1.2 among three controllers.

In order to assess the overall power production performance of three controllers, the annual energy production (AEP) is calculated based on the averaged power at DLC 1.2 and the wind characteristic on the wind farm site. The AEP with controller 1 is 6716.47MWh, while controllers 2 and 3 slightly increase the AEP, with the results of 6762.78MWh and 6764.19MWh, respectively.

5.2. Comparative study through field tests

After validation with simulation testing, the control algorithms are transferred into the PLC program and then integrated into the control system of the studied WT. The field testing site is located in a wind farm on the coast of southern China, in which there are ten 3MW two-blade WTs and seven 2MW three-blade WTs. Before the testing, the control systems of the ten 3MW WTs employ the look-up table torque control algorithm. In order to carry out the field tests, two of the ten machines, named as N15 and N16, are chosen as the testing objectives, because their locations and their power production performance are quite closer to each other. Regarding more power produced by controller 3 than controller 2 in the simulation tests, the updated control algorithm is adopted by N15. Control system 1 is used to update N16. The field tests were carried out in June 2015 and last three weeks.

5.2.1. Field testing results

In the field testing, the control systems are tested in different wind conditions under normal grid operations. Although the power regulation strategy is developed in the control system, this function is inactivated during the tests since in that wind farm, there is no such requirement up to now.

Since different SEZ algorithms are employed by the two control systems, the results with crossing over the SEZ recorded in a 10ms period are shown in Fig. 16 a-b.

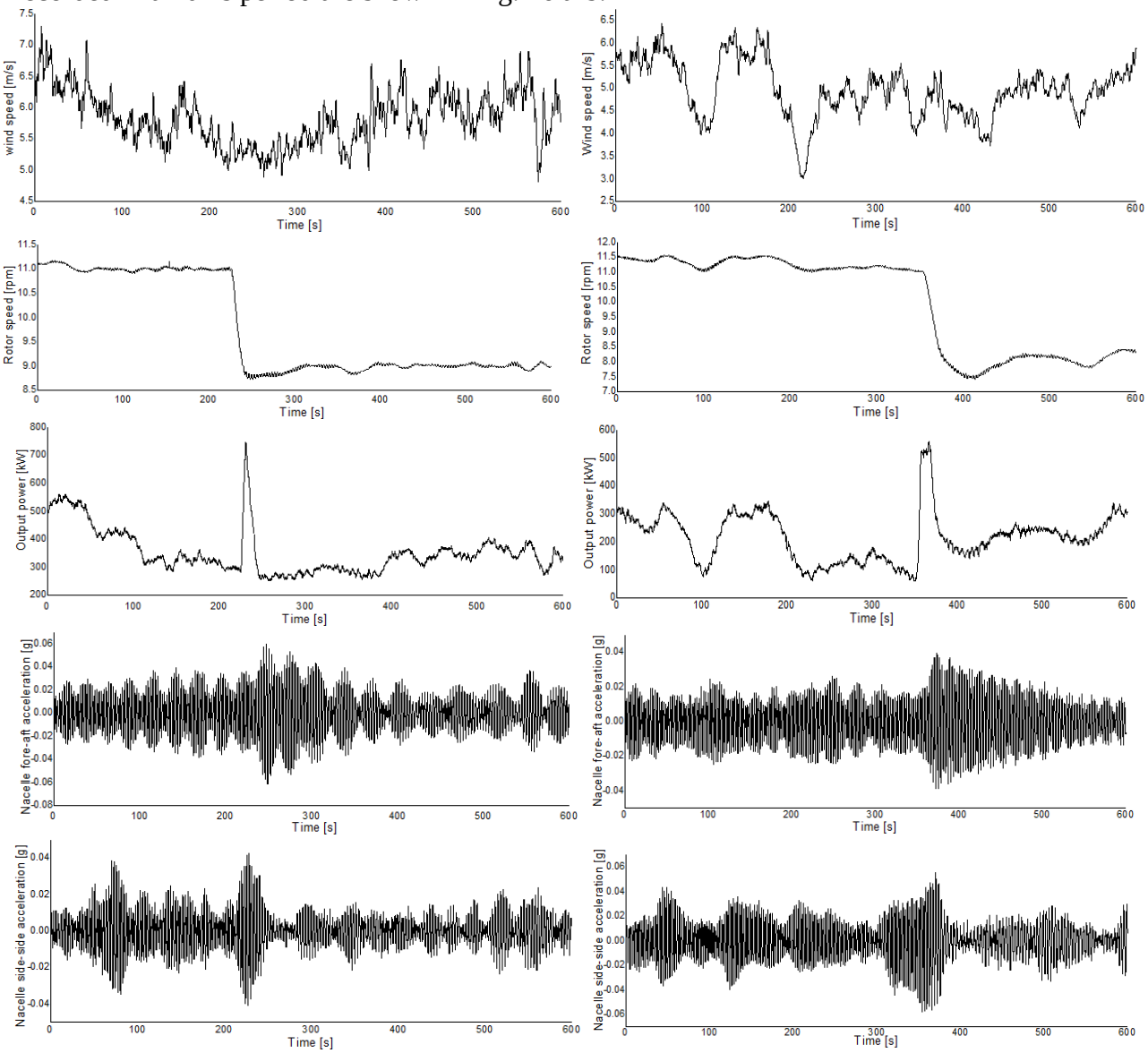

Fig. 16. Crossing-over curves of the SEZ on field testing for: (a) N15 with control system 2 and (b) N16 with control system 1

It can be observed that when the SEZ is crossed over, the output power varies a lot. The peaks of the output power are 750kW and 540kW for N15 and N16, respectively. Meanwhile, the crossing-overs of the SEZ happen at different wind speeds: near 5.5m/s for N15, and 4.5m/s for N16. Besides, both of nacelle fore-aft and side-side accelerations increase along with the transition between two speed zones. The different acceleration amplitude could be the result of varying winds experienced by the whole rotor.

In order to further illustrate different behaviors of two control systems, another field testing result recorded for one day (24h) is presented in Fig. 17. Since the result is with a 10s sampling period, the nacelle acceleration signals are excluded. It is very clear that the rotor speed trajectories and the crossing-over times of the SEZ are different for N15 and N16, while the wind conditions are surprisingly closer to each other.

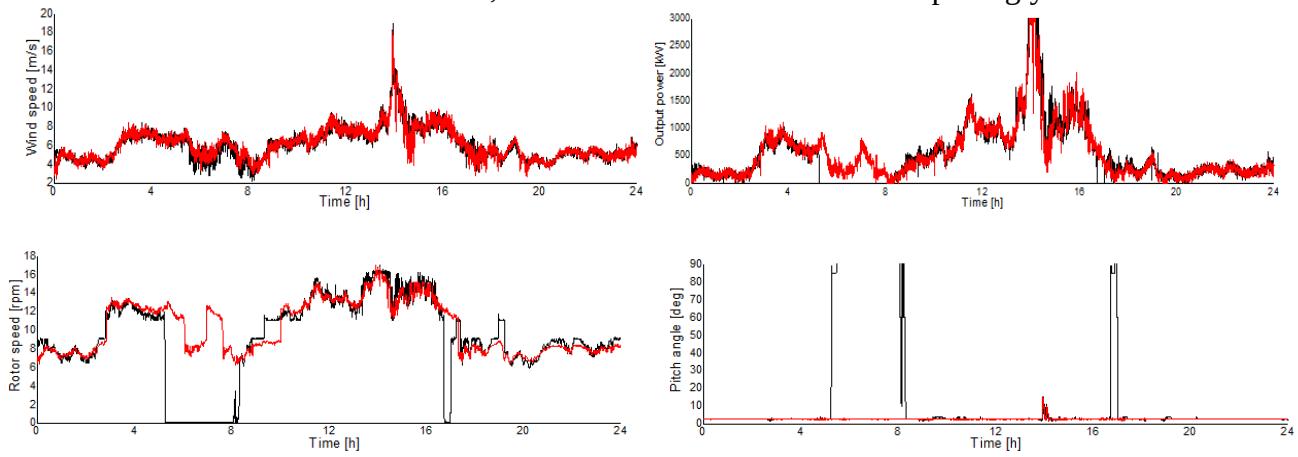

Fig. 17. Field testing curves on one typical day (black curves for N15 and red curves for N16).

5.2.2. Statistics analysis to field testing data

Since the measurement device of tower loads is not equipped in testing WTs, we focus on the data analysis to the power production performance. The data collection is performed between 10th July and 10th August and recorded with 10-min averaged values. Four measurable data (wind speed, rotor speed, output power, and pitch angle) are collected and formed a valid data set after removing the corrupted data. Based on the valid data set, four characteristic curves of N15 and N16 are calculated and illustrated in Fig.18. Three characteristic curves of N15 and N16 are quite different, including rotor speed-wind speed, pitch angle-wind speed, and the TSR-wind speed, while their power-wind speed curves are similar. We observe that one obvious SEZ ranges in 9rpm-11rpm, and the pitch angle of N16 is held at 3 degree, while the pitch angle of N15 varies in the area of 2deg-4deg. For the testing WTs, the pitch angle of 3 degree is the optimal pitch angle (same as the 0 degree illustrated in Fig. 2). Besides, we see that the TSRs of N15 are maintained near the optimal value of 10.5 in the wind speed range of 4m/s-5m/s and 7m/s-9m/s, while N16's TSRs are not constant in the whole wind speed range. Meanwhile, the TSRs of N15 and N16 distribute in different ranges. The TSRs of N15 are scattered between 9.0 and 11.5 at low winds of 4m/s-5m/s, and between 9.8 and 11.2 at high winds of 7m/s-9m/s. By comparison, The TSRs of N16 are more concentrated. It means that the dynamic tracking TSR capability of N15 with control system 2 is inferior to the one of N16 with control system 1.

In order to numerically compare the power capture performance of two control systems, we calculate the averaged output power of N15 and N16. The comparative results shown in Fig. 19 are based on setting the averaged power of control system 1 as the baseline. It is very clear that N15 outputs more power at below rated winds except the wind speed of 7m/s. This result agrees with the characteristic curve of the TSR-wind speed (shown in Fig. 18) well: at 7m/s wind speed, the TSRs of N15 and N16 are closer to the optimal value 10.5, whereas the ones of N16 are much denser. When compared to the simulation result, more power is produced by N15 obviously at low wind range (3m/s-5m/s), while same power-increased trend is presented at high wind range (8m/s-12m/s). These differences can be explained by the fact that the time lengths of simulation and field tests are different; therefore there is uncertainty for power production calculated from

simulation results, especially at low winds. Again, the AEPs of N15 and N16 are calculated based on the field testing results, which are 5763.1MWh and 5695.8MWh, respectively. It is proved that N15 with control system 2 produces more power than N16 with control system 1. However, the AEP obtained from field testing results is less about 15% than the one by simulation calculation, for which the possible reasons could be the wake loss and model tolerance.

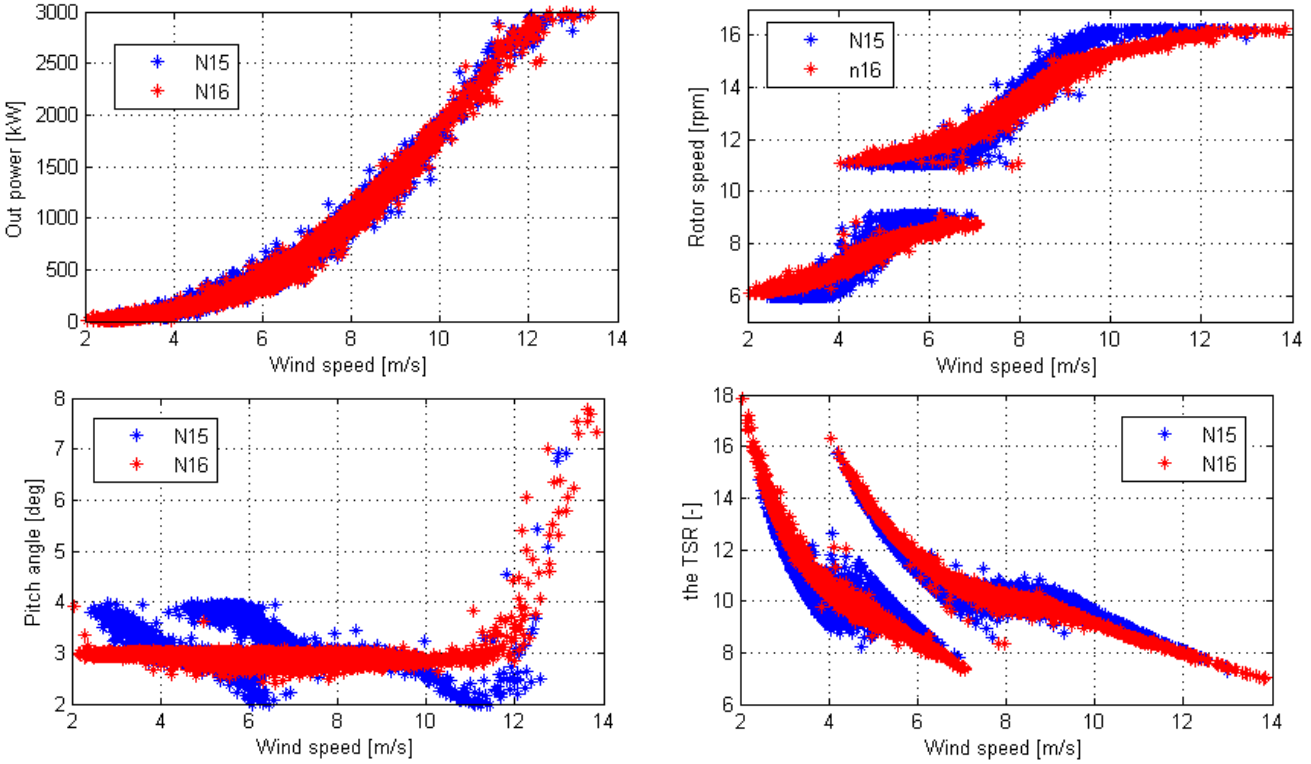

Fig. 18. Comparisons among characteristic curves of N15 and N16

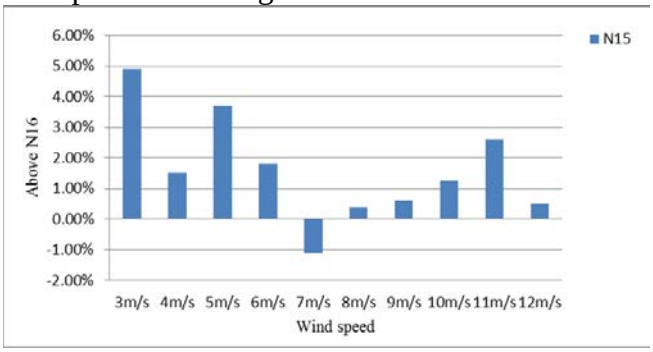

Fig. 19. The averaged output power comparison between N15 and N16.

6. CONCLUSIONS

This paper presents a comparative study on two control systems for a two-blade WT with a SEZ, which is built up to avoid tower resonance. The SEZ of the studied WT is set up and bridged by an appropriate torque control, performed through the boost converter at power optimization operation, in collaboration with the blade pitch control at power regulation operation.

In this paper, two control systems (control system 1 and 2) are developed based on existing torque control strategies, in which three operation strategies have been performed. At power optimization operation, control system 1 employs a conventional look-up table torque control strategy, while control system 2 uses a PI torque controller. In order to guarantee successful crossing-overs of the SEZ under different wind conditions, a hysteresis technique and a variable transition technique are performed in control system 1 and 2, respectively. For the power limitation operation, the two control systems use the same pitch angle controller.

Regarding both the power regulation and the SEZ to be handled at deloaded operation, two power operation modes are divided based on the comparative result between the upper power limit of the SEZ and the power regulation command. In this way, the WT operates in the low speed range with low power command, and in the full speed range with high power command, respectively. As a result, the WT can produce maximal power at the same time maintaining its rotor speed outside the SEZ.

The performances of the WT's control systems have firstly been verified and assessed through simulations with Bladed software. The simulation results illustrate the capability of the developed control systems to control the WT at discussed three operation tasks. At power optimization operation, control system 2 is capable of increasing power production, while there is an uncertainty at low winds. When power production is proved to be influenced by turbulence intensity at low winds, the fatigue loads caused by control system 2 are significantly higher than the one by control system 1. The increased DELs on other components might be negligible, but the increased tower DELs are dominant: a more than 60% increase for tower Mx DEL, and more than 10% for tower My DEL. The detailed numerical results have shown that the increased DELs are mainly contributed by the wind speed range corresponding to the SEZ. Following the simulation tests, the field testing is performed to validate the two control systems and compare the power production performance under power optimization and power limitation operations. The field testing results show that the developed two control systems succeed in controlling the WT to build up and cross over the SEZ. Meanwhile, it is proved the energy capture is enhanced and an increased AEP of 1.1% is achieved by control system 2.

The simulation results also reveal that control system 2 produces more power than control system 1 at power regulation operation. However, in such circumstance, there is a risk of frequent crossing-over the SEZ, when the power regulation command is switched between high power mode and low power mode. Therefore, the WT would suffer from high tower loads. In such case, it is necessary to design a proper wind farm controller to send the proper power command to each WT with the SEZ. This is the subject of future publications.

ACKNOWLEDGMENT

This work was supported by the Fundamental Research Funds for the Central Universities of Central South University under Grant 2015zzts050.

REFERENCES

[1] X. J. Yao, Y. M. Liu, G. D. Liu, Z. X. XING, and J. Q. Bao. Vibration analysis and online condition monitoring technology for large wind turbine. Journal of Shenyang University of Technology 2008; 29(6): 627-632.

[2] G. K. Shan, X. D. Wang, X. J. Yao, and C. C. Zhang. Stability analysis on MW wind turbine. Acta Energiae Solaris Sinica 2008; 29(7): 786-791.

[3] N. Veritas. Guidelines for design of wind turbines. Det Norske Veritas: Wind Energy Department, Risø National Laboratory 2002.

[4] P. Schaak, G. P. Corten, and E. L. Vander Hooft. Crossing resonance rotor speeds of wind turbines. In Proc. EWEC, Madrid, Spain 2003.

[5] E. A. Bossanyi. The design of closed loop controllers for wind turbines. Wind energy 2000; 3: 149-163.

[6] E. A. Bossanyi. Wind turbine control for load reduction. Wind Energy 2003; 6: 229-244.

[7] E. A. Bossanyi. Controller for 5MW reference turbine 2009. [Online]. Avaiable: www.upwind.eu/

[8] J. Licari, J. B. Ekanayake, and N. Jenkins. Investigation of a Speed Exclusion Zone to Prevent Tower Resonance in Variable-Speed Wind Turbines. IEEE Transactions on Sustainable Energy 2013; 4: 977-984.

[9] D. R. Song, J. Yang, M. Dong, Q. Yan, and B. Zhang. Control strategy to avoid tower resonance for two-blade variable-speed wind turbine. Journal of Vibration and Shock 2015; 34: 90-98.

[10]N. W. Miller, JJ. Sanchez-Gasca, W. W. Price, and R. W. Delmerico. Dynamic modeling of GE 1.5 and 3.6 MW wind turbine-generators for stability simulations. In IEEE 2003 Power Engineering Society General Meeting 2003: 1977–1983.

[11]C. Jauch, J. Matevosyan, T. Ackermann, and S. Bolik. International comparison of requirements for connection of wind turbines to power systems. Wind Energy 2005; 8: 295-306.

[12]J. L. Rodriguez-Amenedo, S. Arnalte, and J. C. Burgos. Automatic generation control of a wind farm with variable speed wind turbines. IEEE Transactions on Energy Conversion 2002; 17(2): 279-284.

[13]A. D. Hansen, P. Sorensen, F. Iov, and F. Blaabjeg. Centralised power control of wind farm with doubly fed induction generators. Renewable Energy 2006; 31(7): 935-951.

[14] P. Sorensen, A. D. Hansen, F. Iov, F. Blaabjerg, and M. H. Donovan. Wind farm models and control strategies. Risø National Laboratory, Roskilde, Denmark, Technical Report, 2005.

[15] R. G. De Almeida, E. D. Castronuovo, and J. A. P. Lopes. Optimum generation control in wind parks when carrying out system operator requests. IEEE Transactions on Power System 2006; 21(2): 718-725.

[16] Fernandez L M, Garcia C A, Jurado F. Comparative study on the performance of control systems for doubly fed induction generator (DFIG) wind turbines operating with power regulation. Energy 2008; 33(9): 1438-1452.

[17] GH bladed user manual. Garrad Hassan and Partners Ltd 2009.

[18] M. Soleimanzadeh and R. Wisniewski. Controller design for a wind farm, considering both power and load aspects. Mechatronics 2011; 21: 720-727.

[19] S. Gort, H. D. Doran, K. Weber, H. Norbert. Communication aspects of wind turbine control-architecture redesign. In International Conference on Power Engineering, Energy and Electrical Drives 2011.

[20] J. Yang, D. R. Song, H. Han, P. S. Tong, and L. Zhou. The integrated control of fuzzy logic and model-based approach for variable-speed wind turbine. Turkish Journal of Electrical Engineering & Computer Science 2015; 23(6) : 1715-1734.

[21] N. Wang, K. E. Johnson, and A. D. Wright. Comparison of strategies for enhancing energy capture and reducing loads using LIDAR and feedforward control. IEEE Transactions on Control System Technology 2013; 21: 1129-1142.

[22] Wind turbines – Part 1: Design requirements, IEC 61400-1 International standard (third edition), 2005.